Effects of Membrane Potential on Mechanical Activation in Skeletal Muscle

ANGELA F. DULHUNTY

From the Department of Anatomy, University of Sydney, Sydney, Australia

ABSTRACT The effect of subthreshold depolarization on mechanical threshold was investigated in tetrodotoxin-poisoned mammalian and amphibian skeletal muscle fibers using a two-microelectrode voltage-clamp technique. Mechanical threshold was determined with a 2-ms test pulse. The immediate effect of depolarization was inhibition of the mechanical system. The consequent increase in the test pulse threshold was linearly related to the size of the depolarization and there was, on the average, a 10% increase in threshold for a 10-mV depolarization in mammalian fibers. The duration of the inhibitory period was also related to the size of the depolarization. Inhibition was interrupted by the onset of activation (seen as a reduction in the test pulse threshold), and in rat soleus fibers this occurred within 100 ms with a 20-mV depolarization and within 1 ms with a 40-mV depolarization. Upon repolarization, inhibition decayed within 10 ms. The decay of activation after brief conditioning pulses was initially rapid (on the average, the test pulse threshold recovered to 80% of its control value within 1 ms) and then slow (full recovery took 100–500 ms). After long conditioning pulses, activation often decayed into a period of inhibition. When depolarization (of 20 mV or more) was maintained for several seconds, the fibers became inactivated. Rat extensor digitorum longus and sternomastoid fibers were strongly inactivated by depolarization to −40 mV and the test pulse to +40 mV did not cause contraction.

INTRODUCTION

Mechanical inhibition has been shown to follow depolarization of mammalian skeletal muscle fibers (Dulhunty, 1979 *a*). The term "inhibition" was used to distinguish the small increase in mechanical threshold, seen immediately after a brief depolarizing pulse, from mechanical "inactivation," which is seen during prolonged depolarization (Hodgkin and Horowicz, 1960; Caputo, 1972; Caputo and de Bolanos, 1979) and can block contraction when fully developed. The experiments described in this paper look more closely at the effect of membrane potential on the threshold for mechanical activation, and the conditions required to evoke inhibition, activation, and inactivation. Knowledge of the way in which membrane potential influences mechanical

Address correspondence to Dr. A. F. Dulhunty, Dept. of Anatomy, University of Sydney, N.S.W. 2006, Sydney, Australia.

J. GEN. PHYSIOL. © The Rockefeller University Press · 0022-1295/82/02/0233/19 $1.00 233
Volume 79 February 1982 233–251

activation should prove useful in defining the properties of the voltage-dependent process that governs Ca release from the sarcoplasmic reticulum (SR) in skeletal muscle.

MATERIALS AND METHODS

Biological Preparations and Solutions

The experiments were done on fibers from the following muscles: mouse (QS strain), extensor digitorum longus (EDL), and soleus; rat (Wistar) EDL, soleus, and sternomastoid; and toad (*Bufo marinus*) sartorius. Generally similar results were obtained from each preparation and small species differences will not be described here. For adequate visibility, it was necessary to obtain thin layers of fibers, no more than two to five fibers thick, from the muscles. Mammalian preparations were bathed in a Krebs solution containing: 120 mM NaCl; 3.5 mM KCl; 2.5 mM $CaCl_2$; 1.0 mM $MgCl_2$; 25 mM $NaHCO_3$; 11.0 mM glucose; and 2.0 mM TES [*N*-Tris-(hydroxymethyl)-methyl-2-aminoethanesulphonic acid]. The preparations were bubbled with 95% O_2 and 5% CO_2 (pH = 7.4) and maintained at 30°C. Toad preparations were bathed in a Ringers solution containing: 120 mM NaCl; 2.5 mM KCl; 1.8 mM $CaCl_2$; and 2 mM HEPES (*N*-2-hydroxyethylpiperazine-*N*'-2-ethane-sulphonic acid), pH 7.2, at 20 and 6°C. All solutions contained tetrodotoxin, 5×10^{-7} g/ml, to prevent action potential activity. Temperature was controlled by a heated (or cooled) water jacket surrounding the tissue bath and the temperature of the solution in the bath was monitored by an immersed thermistor probe.

The geometry of the experimental chamber and recording electrodes is shown in Fig. 1 A. The internal dimensions of the tissue bath were 1.5 × 4.5 cm with a depth of 0.8 cm. The base of the bath was filled with 0.3 cm of sylgard (Dow Corning Corp., Midland, Mich.), used to pin the muscle. The preparation was stretched (1.2 × rest length) across a perspex bridge, which supported the fibers for microelectrode penetration. A reference electrode (*r*; Fig. 1 A) was located in the solution 0.5–1.3 cm away from the microelectrodes.

Microelectrodes and Voltage Clamp

KCl-filled glass microelectrodes (resistance, 2–5 MΩ) were used to monitor membrane potential, and either K citrate- or KCl-filled electrodes were used to pass current. The threshold membrane potential for contraction in mammalian fibers was more stable when KCl-filled current electrodes were used. A conventional voltage-clamp circuit, using a ± 140-V operational amplifier, was used to control potential. Changes in command potential had an exponential time-course (time constant = 20 μs). A typical record of membrane potential during a voltage step from −80 to −50 mV is shown in Fig. 1 C (see insert). The total bath current, also shown in the insert in Fig. 1 C, was used to monitor membrane damage during the course of the experiment. A holding potential of −80 mV was used in all experiments. The membrane potential was measured as the potential difference between recording electrode (labeled "v" in Fig. 1 A) and a reference electrode (KCl/agar electrode, labeled "r" in Fig. 1 A).

Determination of Contraction Threshold

The method used to determine contraction threshold was essentially the same as that described previously (Adrian et al., 1969 *a*; Almers and Best, 1976). The preparation was observed on a videomonitor, using a video camera attached to a dissecting microscope, with a final magnification of × 500. The microelectrodes were placed as

shown in Fig. 1 B. The separation between the electrodes was normally 0.5–1.0 times the diameter of the fiber (fibers from various muscles used in the experiments had a range of diameters from 50 to 120 μm). Contraction was observed along the edge of the fiber, opposite the current electrode, in the area indicated by the shaded part in Fig. 1 B. The errors involved in assumption of controlled membrane potential in this area are discussed below. The size of a depolarizing pulse was increased in 2-mV steps

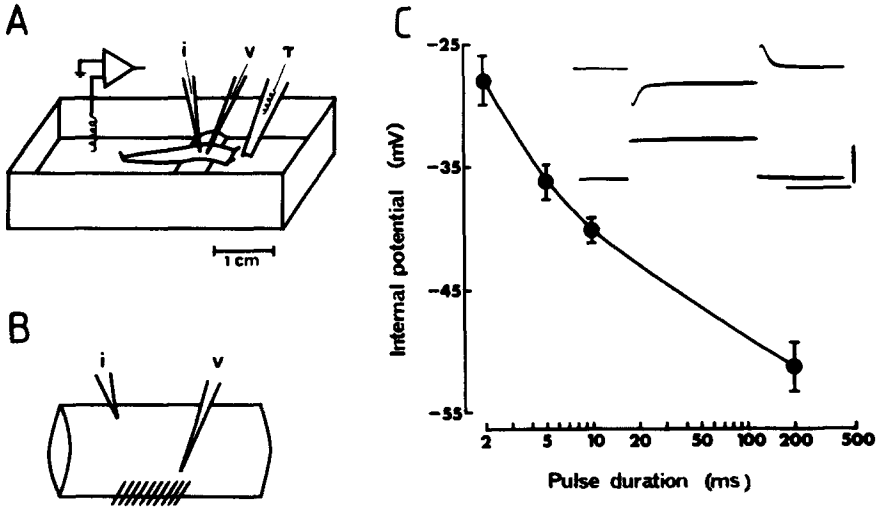

FIGURE 1. Recording setup and strength duration curves. (A) arrangement of the preparation, current (i), and voltage (v), microelectrodes, reference electrode (r), and ground electrodes. The tissue bath has been drawn to scale. (B) arrangement of the current (i), and voltage (v), microelectrodes in a single muscle fiber. The shaded area shows the region of the fiber in which contraction was observed. (C) average strength duration curve for 37 rat soleus fibers used in this series of experiments. Complete curves were not obtained for each fiber, but each symbol represents average data from at least seven fibers. Bars depicting ± 1 SEM are shown. The insert shows total bath current (upper trace) and membrane potential (lower trace) recorded from a fiber at the end of a series of threshold determinations. The fiber had an initial resting potential of −60 mV and was held at −80 mV during the experiment. The holding current at the end of the run was 200 nA. The fiber had a diameter of 75 μm and the electrode separation was 60 μm. Horizontal calibration, 2 ms; vertical calibration, 500 nA (upper trace) and 20 mV (lower trace).

until movement of the fiber edge was detected. Then the pulse was reduced in 0.2-mV steps until contraction was no longer visible. The membrane potential during the pulse to just below contraction threshold was recorded and could normally be reproduced in repeated determinations with an accuracy of ± 0.2 mV. An average strength-duration curve for the contraction threshold of rat soleus fibers, used in the experiments reported below, is shown in Fig. 1 C. Small changes in threshold were often observed during a series of trials on one fiber. However, the changes were sufficiently slow to allow appropriate corrections to be made to control pulses (see below). Results of a trial were rejected if the point of contraction moved or if the threshold potential for a control pulse varied by more than 1 mV.

Problems with Membrane Potential Control

The techniques used have a number of inherent problems that introduce errors into the determination of a true contraction threshold, but do not influence relative changes in contraction threshold reported below.

A problem with the voltage-recording system shown in Fig. 1 A is the series resistance through the solution, between the fiber membrane and the reference electrode. A fraction of the imposed voltage step will appear across the series resistance, and this fraction may be as great as 10% (in the worst case) of a change in steady-state membrane potential. The fraction is greater when brief (<10 ms) pulses are used.

Another problem is associated with nonuniformities in the membrane potential around the current electrode. When a depolarizing step is applied to the voltage-clamped muscle fiber, the membrane potential at the current electrode is more positive than the potential at the voltage electrode, and as the depolarization approaches contraction threshold, contraction is first apparent around the current electrode (Adrian et al., 1969 *b*). The effect of this problem was reduced by focusing the microscope on the edge of the fiber (shaded area; Fig. 1 B). Movement around the current electrode could normally be distinguished from contraction at the edge of the fiber. Fibers demonstrating gross movement at the current electrode were rejected. If movement around the current electrode influenced the edge of the fiber, the contraction threshold would have been underestimated.

The spread of nonuniformities in membrane potential away from the current electrode depends upon a number of factors that include the space constant and radius of the fiber, the angular separation between the microelectrodes, and the depth of the electrodes within the fiber. Quantitative analyses of this problem are presented by Adrian et al. (1969 *b*) and Eisenberg and Johnson (1970). The latter authors include tables that can be used to estimate the deviation of the membrane potential from the potential at the voltage electrode. The deviation of the steady-state membrane potential in the shaded region of Fig. 1 B is <1% (assuming λ = 1 mm, radius = 30 μm, and electrode separation greater than the radius). The deviation is greater for brief pulses. For example, the space constant is 500 μm for a 1-ms pulse (equivalent frequency = 500 Hz; effective capacity = 2 μF/cm^2; Eisenberg and Johnson, 1970), and the deviation from the recorded membrane potential increases to 2%. The errors introduced by nonuniformities in membrane potential became smaller with distance from the current electrode. Unfortunately, problems arising from cable decrement along the fiber become apparent as the separation between the electrodes is increased, and this problem is more significant when brief pulses are used and the effective space constant is less than it is for long pulses.

One further problem is that a brief pulse may depolarize the T tubule membrane less than the surface membrane if an "access" resistance (Valdiosera et al., 1974) at the mouth of the T system causes a delay in depolarization of the T tubule membrane. There are no data available to estimate the value of an "access" resistance in mammalian fibers, so the error introduced is difficult to assess.

As mentioned previously, the results presented in this paper are based on observations of relative changes in contraction threshold. The experimental conditions were such that errors in the determination of the precise contraction threshold remained constant and should not have affected the results. The errors with brief pulses may have been significant when the effects of conditioning pulses of different duration were compared (see *Two-Pulse Technique,* described below). Individual cases will be discussed as they arise in Results.

Damage to the membrane during penetration of the voltage electrode can also lead to nonuniformity in membrane potential. Adrian et al., (1969 *b*) and Costantin (1974) describe preliminary contraction of one to three sarcomeres around the voltage electrode when voltage steps of increasing amplitude were applied to the fiber. This effect was not resolved with the dissecting microscope used in the experiments reported here.

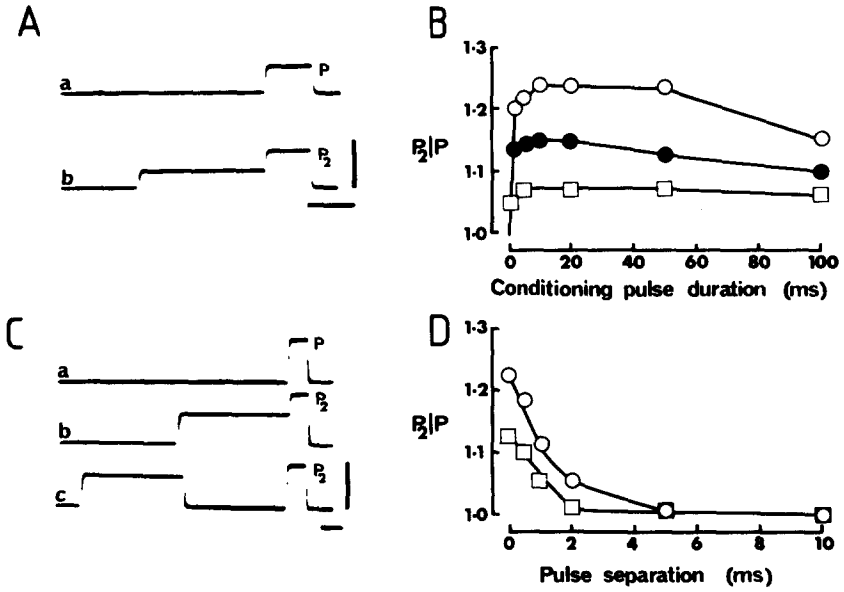

FIGURE 2. The inhibitory effect of subthreshold depolarization. Records in A and C illustrate voltage steps used to obtain some data shown in B and D, respectively. A: *a*, test pulse alone (P); *b*, test pulse (P_2), preceded by a 20-mV conditioning pulse of 5.0 ms. B: test pulse ratio, P_2/P, against the duration of conditioning pulses for one EDL fiber (resting potential, V_m, = −65 mV; holding potential, V_H = −79.4 mV; temperature, T, = 31°C). The fiber was inhibited ($P_2/P>1$) by conditioning pulses of 5 (□), 10 (●), and 20 mV (○). C: *a*, test pulse alone (P); *b* and *c*, test pulse (P_2), separated from a 5-ms, 40-mV conditioning pulse by 0 and 5.0 ms. D: test pulse ratio, P_2/P, against pulse separation for one rat soleus fiber (V_m = −60 mV; V_H = −80.5 mV; T = 29.3°C). The conditioning pulse was 5 ms and 34 mV (○), or 20 mV (□). For A and C, the horizontal calibration is 2 ms and the vertical calibration is 50 mV.

Two-Pulse Technique

A two-pulse technique was used to determine the effect of subthreshold depolarization on contraction threshold as shown in Fig. 2 A. A 2-ms test pulse was immediately preceded by a subthreshold conditioning pulse. The threshold potential for the test pulse, P_2, was compared with the threshold for the test pulse alone, P, and the ratio P_2/P was used as an index of the effect of the conditioning pulse on contraction threshold. The recovery of a fiber from a brief depolarization was determined using the pulse sequence shown in Fig. 2 C. A test pulse was applied at various intervals

after the termination of a subthreshold conditioning pulse. P_2 was again compared with the threshold for the test pulse alone and the ratio P_2/P was used as an index of the recovery of the fiber from the conditioning pulse.

There was a remote possibility that the "inhibition" described in this paper might arise from an artefact of the microelectrode voltage-clamp technique used. However, the phenomenon has been observed in fibers under gap voltage clamp. Using tendon-terminated cut segments of frog semitendinosus fibers voltage-clamped by the single-gap method (Kovacs and Schneider, 1978), Horowicz and Schneider (personal communication) have observed that at 2–5°C, the fiber movement produced by a slightly supra-rheobase 70-ms test pulse could be decreased when the test pulse was immediately preceded by a somewhat smaller 65–130-ms prepulse that was itself below rheobase for detectable fiber movement.

RESULTS

Short-Term Effects of Depolarization on Contraction Threshold

The two-pulse technique described in Methods was used to evaluate the short-term effects of depolarization on contraction threshold. The effect of the subthreshold conditioning pulse was described as inhibition (when it caused an increase in test pulse threshold and $P_2/P > 1$) or activation (when it caused a decrease in test pulse threshold and $P_2/P < 1$).

Mechanical Inhibition during Weak Depolarizing Pulses

The phenomenon of inhibition was clearly demonstrated by observing the blocking effect of a subthreshold conditioning depolarization (e.g., 20 mV for 10 ms). A fiber that clearly contracted when a test pulse was just greater than threshold would not contract when the test pulse was preceded by a conditioning depolarization. Conversely, a test pulse that was just subthreshold when applied with a weak conditioning depolarization would evoke a vigorous contraction when applied alone. The contraction in this case is often strong enough to dislodge the microelectrodes.

Inhibition was seen most clearly with the conditioning depolarizations of 5–25 mV. The symbols in Fig. 2 B show the inhibitory effects of 5-, 10-, and 20-mV conditioning pulses lasting 5–100 ms. The decline in inhibition apparent with longer pulses (see Fig. 2 B) was probably due to the onset of subthreshold activation, which was seen with maintained depolarization (see later results). The recovery of a fiber from inhibition caused by 20- and 30-mV conditioning pulses lasting 5 ms is shown in Fig. 2 D. The test pulse threshold remained higher than normal for several milliseconds after the conditioning pulse was terminated. The time-course of decay of inhibition cannot be assessed from the data shown in Fig. 2 D because the membrane potential during the decay period is uncertain.

It is clear that the increase in test pulse threshold depended on the size of the conditioning depolarization. The threshold of the fiber shown in Fig. 2 B increased by 7% after a 5-mV depolarization (open squares) and by 20% after a 20-mV depolarization (open circles). The voltage dependence of the thresh-

old increase is shown in Fig. 3, where the test pulse ratio has been plotted against membrane potential. On the average, there was a 10% increase in threshold for a 10-mV reduction in membrane potential between −80 and −50 mV. Activation became apparent when EDL fibers were depolarized beyond −50 mV (for 5–10 ms) and thus the curve in Fig. 3 has not been extended beyond that membrane potential. The triangles in Fig. 3 show average data obtained from 20 toad sartorius fibers at 20°C. The increase in test pulse threshold after conditioning depolarization was found in these fibers, but was smaller and less easy to demonstrate than it had been in mammalian fibers.

The increase in threshold shown in Figs. 2 and 3 might have been the result of a voltage-dependent conductance change in the T tubule membrane. Chloride conductance is the dominant conductance in the mammalian T

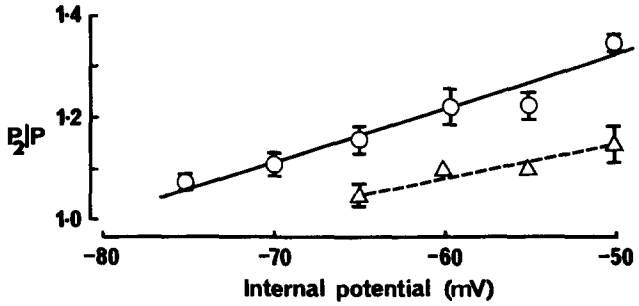

FIGURE 3. The voltage dependence of inhibition. The test pulse ratio, P_2/P (see Fig. 2 A), measured during the plateau phase of inhibition (i.e., 10–20 ms after depolarization; see Fig. 2 A) is plotted against the membrane potential during the conditioning depolarization. The open circles show average data (± 1 SEM) from 10 mouse EDL fibers at 30°C. The open triangles show data from 21 toad sartorius fibers at 20°C. Straight lines have been drawn through the average data.

system (Palade and Barchi, 1977; Dulhunty, 1979 *b*) and hence removal of chloride ions should eliminate the increased threshold effect if it were due to a change in chloride conductance, or enhance the effect if it were due to some other conductance system. Six rat soleus fibers were studied in a solution in which the NaCl was replaced by an equimolar concentration of TEA bromide (Palade and Barchi [1977] showed that bromide conductance is <20% of chloride conductance in rat diaphragm). A pulse protocol similar to that shown in Fig. 2 A was used and the increase in test pulse threshold after a conditioning depolarization was similar to that shown in Fig. 2 B and was identical to that recorded in five other fibers after the muscle had been returned to the normal Krebs-Ringer solution.

The increase in threshold is therefore independent of T tubule space constant and the results suggest that a voltage-dependent inhibitory process is "turned on" by depolarization.

Mechanical Activation during Strong Depolarizing Pulses

The data in Fig. 2 B showed evidence of the onset of activation (i.e., a reduction in P_2/P) after long conditioning pulses. Depolarization to membrane potentials more positive than the rheobase potential caused contraction ($P_2/P = 0$) if the duration of the depolarization exceeded a critical value (shown on the strength duration curve in Fig. 1 C) and the test pulse threshold fell steeply as the duration of the conditioning pulse approached that value (Fig. 4 A and B). Small changes in conditioning pulse size could dramatically shift

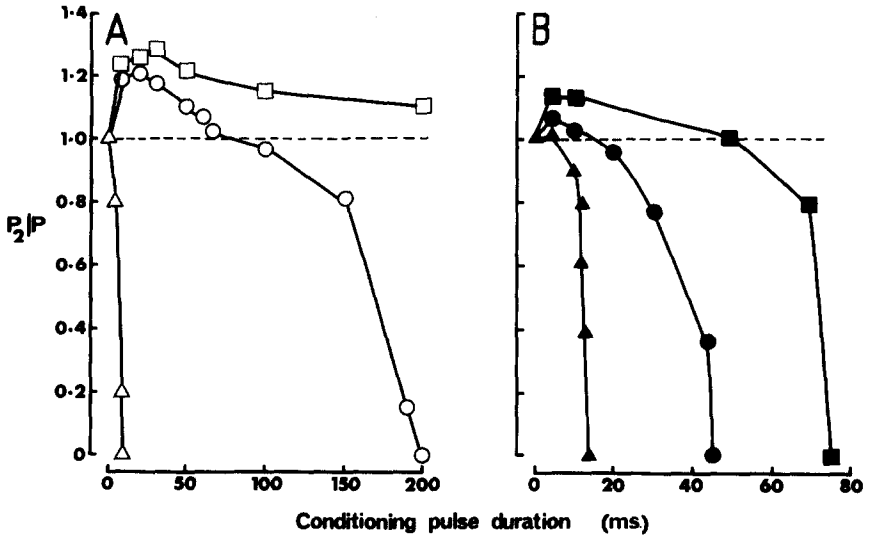

FIGURE 4. The onset of activation with strong conditioning depolarization (i.e., steps >25 mV). A is a graph of test pulse ratio, P_2/P plotted against conditioning pulse duration for a rat soleus fiber ($V_m = -70$ mV; $V_H = -80$ mV; T = 29.4°C). The test pulse P_2 was applied immediately after conditioning pulses of 25 (□), 30 (○), and 40 mV (△). B is a graph of test pulse ratio, P_2/P, plotted against conditioning pulse duration for a rat EDL fiber ($V_m = -62$ mV; $V_H = -80.7$ mV; T = 29.2°C). The test pulse P_2 was applied immediately after conditioning pulses of 34 (■), 39 (●), and 42 mV (▲). The lines have been drawn to connect the data points. The broken lines indicate the level at which $P_2/P = 1$.

the time at which test pulse threshold began to decline. The steep fall in test pulse threshold, as conditioning pulses approached their threshold duration, is consistent with the steep voltage dependence of tension (Hodgkin and Horowicz, 1960; Caputo and de Bolanos, 1978; Dulhunty, 1980). The data are also consistent with the observation that long (50 ms) pulses set 1–2 mV below contraction threshold do not reduce test pulse amplitude by more than 50% (Adrian et al., 1969 *a*; Costantin, 1974). The data suggest that there is a voltage-dependent delay in the onset of activation, but it is difficult to estimate how much of this delay is due to a delay in the excitation-contraction coupling mechanism and how much is due to the effect of inhibition.

When the conditioning pulse was sufficiently strong (i.e., >40 mV in soleus fibers or 55 mV in EDL fibers) the onset of activation was so rapid that inhibition was not obvious (see Fig. 5 A). The onset of activation with strong conditioning pulses occurred at times that were <1 ms and thus interpretation is made difficult by the uncertainty of the membrane potential during this time.

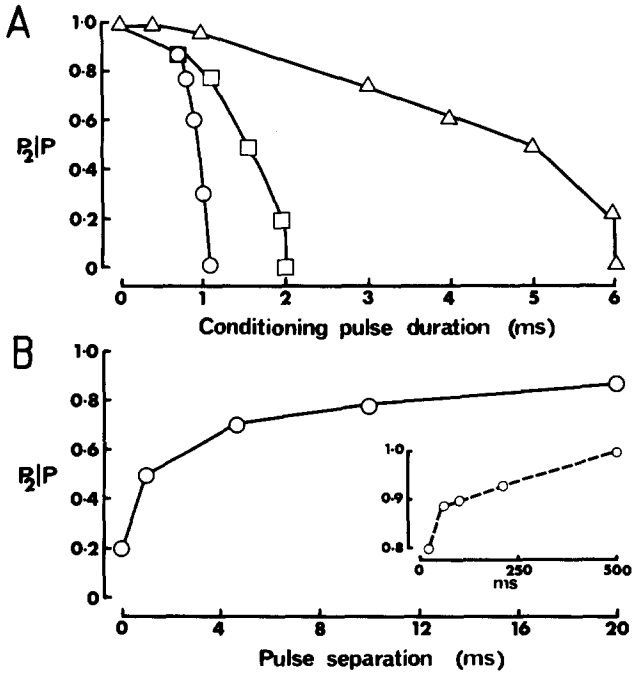

FIGURE 5. The onset and decay of activation induced by strong conditioning depolarization. The data in A were taken from the same soleus fiber used in Fig. 4 A. The test pulse ratio, P_2/P, is plotted against conditioning pulse duration and the test pulse, P_2, was applied immedately after 40 (△), 50 (□), and 60 mV (○) conditioning pulses. The data in B was taken from a different rat soleus fiber (V_m = −60 mV; V_H = −80.5 mV; T = 29.0°C). The test pulse ratio, P_2/P, is plotted against the separation between the termination of a 1.0 ms conditioning pulse to −20 mV (threshold for a 1.0 ms pulse was −16.1 mV) and the test pulse P_2. The insert in B shows the slow decay of activation seen with pulse separations between 10 and 500 ms. The lines in A and B have been drawn to connect data points.

Recovery of Fibers from Depolarization

Fibers recovered rapidly from depolarization and the most interesting phase of recovery occurred within 10 ms of the termination of the conditioning pulse. The membrane potential was not well controlled during this period (see Methods). The results are presented with this reservation in mind because they reveal some interesting aspects of the interaction between activation and inhibition. A more quantitative treatment of the data is probably not justified.

The recovery of a fiber from a strong 1-ms depolarization (set to a membrane potential that was 1 mV below contraction threshold) is shown in Fig. 5 B. The profile of recovery was similar to that described by Adrian et al. (1969) and by Costantin (1974). Activation decayed rapidly and then slowly: the test pulse recovered to 80% of its control value after 10 ms but took 500 ms to recover fully (see insert in Fig. 5 B).

Recovery of Fibers from Brief Conditioning Pulses of Different Amplitudes

Generally, the time-course of decay of activation could be easily followed after 1 ms conditioning pulses to membrane potentials that were 1–3 mV below contraction threshold (see Fig. 5 B and Fig. 6 A and B, open circles). The decay of activation could not be followed after smaller depolarizing pulses of the same duration because inhibition became apparent and distorted the records as shown for the two fibers in Fig. 6 A and B (similar families of curves were obtained from seven other rat soleus fibers, three rat EDL fibers, and 10 mouse EDL fibers). 1-ms conditioning pulses set to 70% or less of their threshold potential were normally followed by a period of inhibition (open triangles in Fig. 6 A and B), which decayed within 5–10 ms. Conditioning pulses that were 70–90% of threshold were followed by a simple combination of activation and inhibition (Fig. 6, filled circles). A period of inhibition, 0.5–1.0 ms after the conditioning pulse, declined into a period of activation that subsequently decayed with a time-course that was parallel to the slow decay phase of activation (open circles).

The summation of activation and inhibition shown in Fig. 6 makes it difficult to interpret the apparently simple decay of activation after brief pulses set close to contraction threshold. It seems likely that inhibition influences the time-course of the rapid phase of activation decay, but it is difficult to assess the extent of this influence. Since inhibition is minimal after 10 ms it presumably does not influence the time-course of the slow decay of activation. The simple combination of activation and inhibition after depolarizing pulses suggests that there is summation of two independently decaying processes.

Recovery of Fibers from Strong Conditioning Pulses of Different Duration

It was difficult to follow the decay of activation after conditioning pulses that were longer than 1 ms. Fig. 7 A shows the recovery of a fiber after 1.0-, 2.0-, and 5.0-ms pulses set to 90–94% of their threshold potentials. Activation decayed in a simple manner after the 1-ms pulse (open triangles) but was swamped by inhibition after the 2- and 5-ms pulses (circles). Similar results were obtained in 20 other mammalian fibers. When the size of a 5-ms conditioning pulse was increased to 98% of its threshold value (Fig. 7 B) there was some activation at the end of the pulse but this quickly decayed into inhibition. Qualitatively similar results were obtained using 10- (Fig. 7 C), 30-, and 50-ms conditioning pulses, although it became progressively more difficult to see activation as pulse length increased (and pulse amplitude

decreased). The slow phase of the decay of activation was apparent in fibers recovering from long pulses (Fig. 7 A–C).

The decay of activation was more easily followed in toad muscle fibers, where inhibition is relatively less (see Fig. 3 above). The open triangles in Fig. 7 D show the recovery of one fiber from a 10-ms pulse set to 97% threshold. When the pulse size was reduced to 92% threshold (filled circles) inhibition was recorded. The decay of inhibition at 7.5°C (Fig. 7 D) was very much

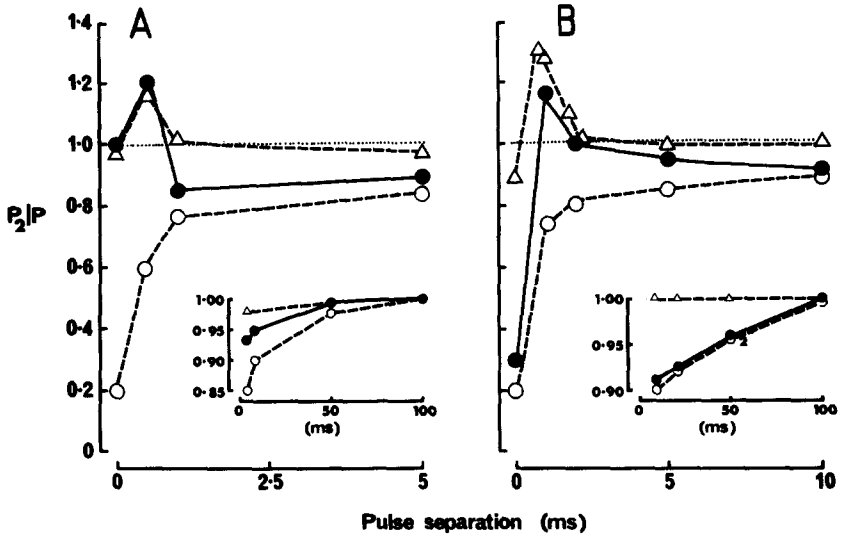

FIGURE 6. The recovery of fibers from brief conditioning pulses of different amplitudes. The test pulse ratio, P_2/P, is plotted against the separation between the termination of 0.5 ms conditioning pulses and the test pulse P_2. The data in A were taken from a mouse EDL fiber (V_m = −82 mV; V_H = −80.7 mV; T = 29.1°C) after conditioning pulses of 52 (○) (90% threshold), 45 (●) (75% threshold), and 40 mV (△) (67% threshold). The data in B were taken from rat soleus fibers. The triangles and filled circles show data from one fiber (V_m = −65 mV; V_H = −80.1 mV; T = 30.3°C) after conditioning depolarizations of 98 (●) (91% threshold) and 80 mV (△) (74% threshold). The open circles show data from a different fiber (V_m = −68 mV; V_H = −80.0 mV; T = 30.6°C) after conditioning depolarization of 54 mV (○) (96% threshold). The inserts A and B show recovery up to 100 ms after the depolarization. Solid and broken lines have been drawn connecting the data points. The dotted lines indicate the level at which P_2/P = 1.

slower than the decay at 20°C (which was similar to that in mammalian fibers at 37°C; see Fig. 2).

The dominant effect of inhibition after long pulses in mammalian fibers (Fig. 7 A–C) would occur if either inhibition was greater or activation was less than that evoked by strong brief pulses. Costantin (1974) found that activation decayed more slowly after long pulses. If the same is true for mammalian

preparations, then inhibition must also be stronger after long pulses, and must be sufficiently strong to hide the effect of the slower decay of activation.

Effect of Prolonged Depolarization on Mechanical Threshold

The mechanical threshold was determined, using a 2-ms test pulse, at various intervals after a change in the resting membrane potential (holding potential). Each threshold determination took about 15 s to complete and the initial

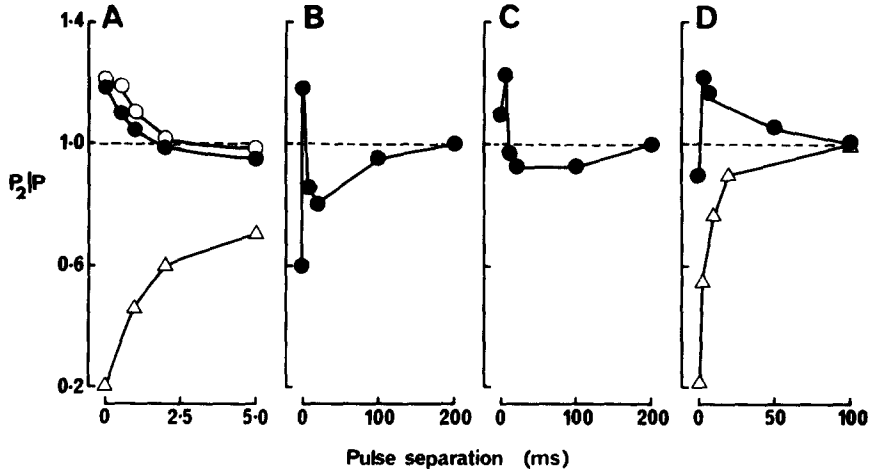

FIGURE 7. The recovery of fibers from strong conditioning pulses of different duration. The test pulse ratio, P_2/P, is plotted against the separation between the termination of the conditioning pulse and the test pulse, P_2. The data in A were taken from a rat soleus fiber (V_m = −60 mV; V_H = −80.5 mV; T = 29.0°C) after 1 (△) (60 mV; 94% threshold), 2 (●) (40 mV; 93% threshold), and 5 ms (○) (36 mV; 90% threshold) conditioning depolarizations. The data in B were taken from a mouse EDL fiber (V_m = −68 mV; V_H = −80.4 mV; T = 29.2°C) after a 5-ms, 40-mV (90% threshold) conditioning depolarization. The data in C were taken from a rat soleus fiber (V_m = −68 mV; V_H = −80.3 mV; T = 30.5°C) after a 10-ms, 36-mV (94% threshold) conditioning depolarization. The data in D were taken from a toad sartorius fiber (V_m = −70 mV; V_H = −80 mV; T = 7.5°C) after 10-ms conditioning depolarizations of 41 (△) (97% threshold) and 35 mV (●) (92% threshold). The broken lines indicate the level at which P_2/P = 1.

effects of potential changes on mechanical threshold (described above) could not be resolved. Average steady-state threshold values (recorded 3–10 min after the change in membrane potential) have been plotted against membrane potential in Fig. 8. A small reduction in membrane potential caused sub-threshold activation (which is consistent with the trends shown in Fig. 3 B above). Contraction threshold reached a minimum value (Fig. 8 A and B) when the holding potential was 10 mV more positive than the initial resting potential (recorded when the microelectrode first entered the fiber; −67.9 ±

2.5 mV for 10 rat fibers and −81.6 ± 1.6 mV for 24 toad fibers). A further reduction in membrane potential led to an increase in test pulse threshold. Rat EDL and sternomastoid fibers could not be activated by a 2-ms test pulse to +40 mV when the membrane potential was depolarized beyond −40 mV.

The time-courses of changes in activation threshold are shown in Fig. 9. The onset of subthreshold activation (Fig. 9 A) is slow when compared with the activation curves shown previously (see Fig. 4 B). However, activation does become much slower when the size of the depolarization is reduced. The time-course of recovery from activation was too fast to be resolved (Fig. 9 B). The increase in test pulse threshold, seen at more positive membrane potentials, was slow and was normally preceded by a period of activation (Fig. 9 C).

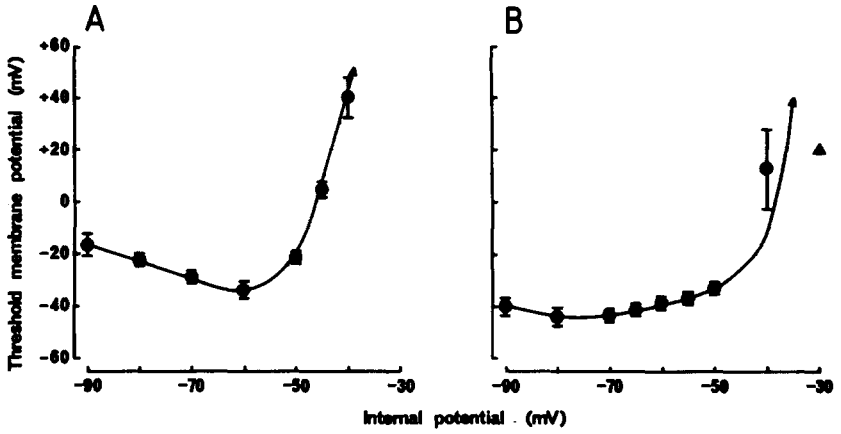

FIGURE 8. The effect of prolonged depolarization on mechanical threshold. Average data (mean ± 1 SEM) from 8 rat EDL fibers (A) and 16 toad sartorius fibers (B) are shown. Mechanical threshold, measured 3 min after a change in membrane potential, is plotted against the new membrane potential. The lines have been drawn through the average data. In rat EDL fibers (A) depolarization beyond −40 mV caused a rapid increase in test pulse threshold to potentials greater than +120 mV. All changes in threshold shown in the graph were reversed when the membrane potential was returned to −80 mV.

The recovery of mechanical threshold after repolarization was also relatively slow (Fig. 9 D), taking several minutes to complete. The slow increase in test pulse threshold (Fig. 9 C) and its decay (Fig. 9 D) demonstrate a time dependence that is similar to that of mechanical inactivation (Hodgkin and Horowicz, 1960; Caputo, 1974; Caputo and de Bolanos, 1979; Dulhunty, 1980) and is probably a reflection of the same mechanism.

Caputo and de Bolanos (1979) found that a long conditioning depolarization could reduce the tension response to a test depolarization without itself causing a contraction. This result might be interpreted to mean that inactivation can proceed without activation and hence that the two processes are independent. In the experiments reported here, inactivation was always

preceded by activation (in mammalian and amphibian preparations), although the latter was subthreshold if the depolarizing step was sufficiently small. In the experiment illustrated in Fig. 10, the membrane potential was changed from −80 to −35 mV in 5-mV steps. Subthreshold activation (reduction in test pulse threshold) preceded the development of inactivation after each depolarizing step.

DISCUSSION

The experiments reported above show that the threshold membrane potential for contraction changes in a complex way when a muscle fiber is depolarized.

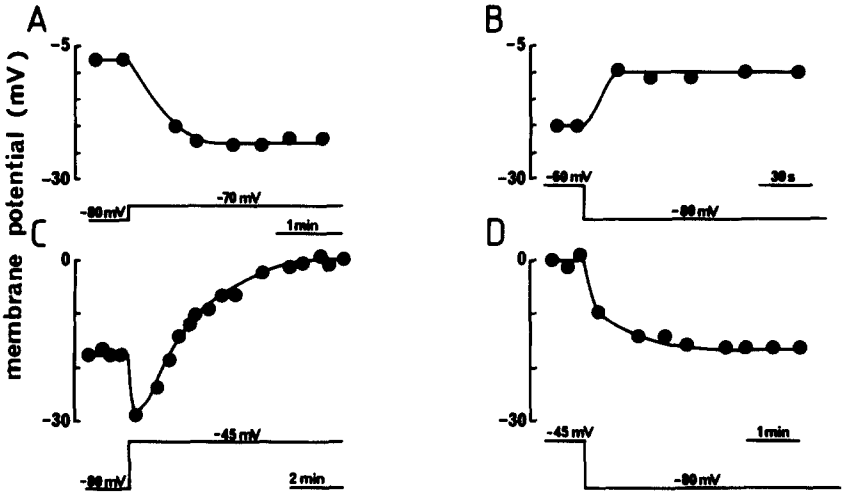

FIGURE 9. The time-course of mechanical threshold changes during prolonged depolarization in a rat white sternomastoid fiber (V_m = −76 mV; V_H = −80.1 mV; T = 29.8°C). Step changes in holding potential are indicated under each graph. The threshold membrane potential (for a 2-ms test pulse) is shown on the vertical axes. A: development of subthreshold activation with depolarization from −80 to −70 mV. B: recovery from subthreshold activation with repolarization from −60 to −80 mV. C: development of inactivation with depolarization from −80 to −45 mV. D: recovery from inactivation with repolarization from −45 to −80 mV. Time scales are indicated beneath each graph.

For example, a mouse EDL fiber depolarized from −80 to −60 mV is initially inhibited and the contraction threshold increases to a maximum value that is maintained for 50–100 ms. After that time subthreshold activation causes a reduction in the threshold potential that may last for several seconds. Finally, inactivation becomes effective and the threshold potential once again increases. Strong depolarization (e.g., from −80 to −20 mV) causes a rapid increase in activation and the weaker influence of inhibition is not observed.

The following comparison of aspects of inhibition and inactivation suggest that they are not a manifestation of the same process (as suggested previously in Dulhunty, 1979 *a*). Inhibition approaches a maximum value with a rate

that is at least five orders of magnitude faster than the rate of inactivation. In marked contrast to inactivation, inhibition was never strong enough to block activation by the 2-ms test pulse. Finally, inactivation and inhibition exhibit quite different fiber type dependences. Inactivation proceeds five times more slowly in soleus fibers than in EDL fibers (Dulhunty, 1980), whereas the kinetics of inhibition in the two muscles vary by only 20% (unpublished observations).

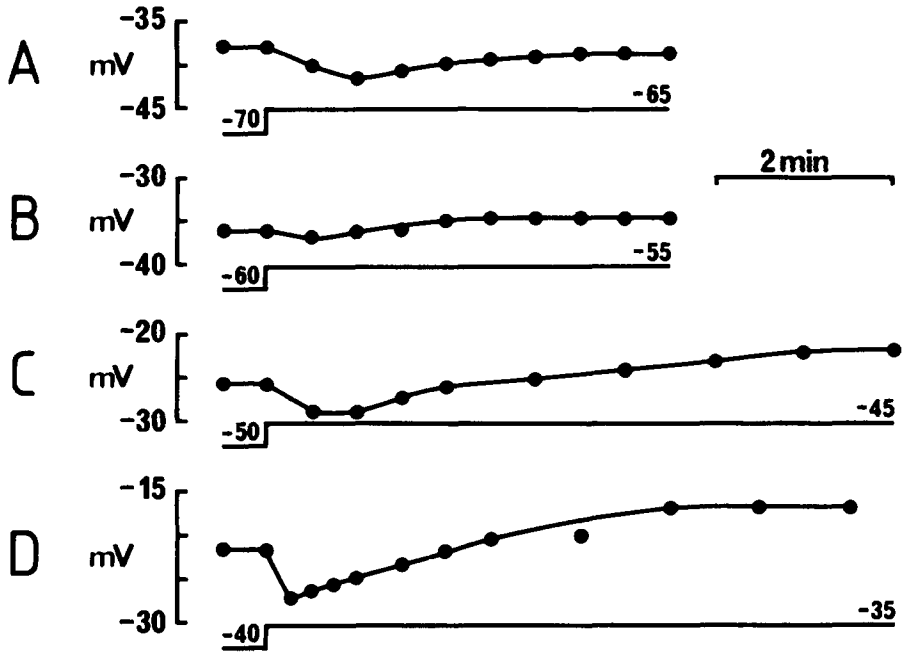

FIGURE 10. Development of inactivation preceded by subthreshold activation in a toad sartorius fiber (V_m = −85 mV; V_H = −90 mV; T = 23.1°C), depolarized from −70 to −35 mV in 5-mV steps. The step changes in membrane potential are shown beneath each graph. The threshold membrane potential (for a 2-ms test pulse is shown on the vertical axis). A: depolarization from −70 to −65 mV. B: depolarization from −60 to −55 mV. C: depolarization from −50 to −45 mV. D: depolarization from −40 to −35 mV. Time calibration is 2 ms.

The possible origins of inhibition and inactivation pose interesting questions. It is unlikely that inactivation is due to either Ca depletion from the SR or to Ca pump activity (Caputo, 1972; Dulhunty, 1980); it may be a property of the process coupling depolarization of the T tubule membrane with Ca release from the sarcoplasmic reticulum (SR). It is commonly thought that Ca release is triggered, either directly or indirectly, by the reorientation of a voltage-sensitive molecule located in the T tubule membrane. The movement of the voltage-sensitive molecule is probably reflected in asymmetric capacitive

currents (Schneider and Chandler, 1973), which demonstrate inactivation kinetics (Chandler et al., 1976; Adrian et al., 1976), and it is tempting to suggest that mechanical inactivation is a result of inactivation of the T tubule voltage sensor. Ca current inactivation might also contribute to mechanical inactivation, provided that the SR Ca conductance is similar to other voltage-sensitive Ca conductances (Adams et al., 1980; Sanchez and Stefani, 1978) and is not directly "gated" by the T tubule voltage sensor (Chandler et al., 1976).

Inhibition has not been reported in previous activation studies and its origin is open to speculation. If it is assumed that there is only one rapid functional link between the T system and SR, then inhibition must arise within the T tubule membrane. One simple model for inhibition and inactivation (which is consistent with previous models for the mechanical activation system; Caputo, 1972; Chandler et al., 1976) is:

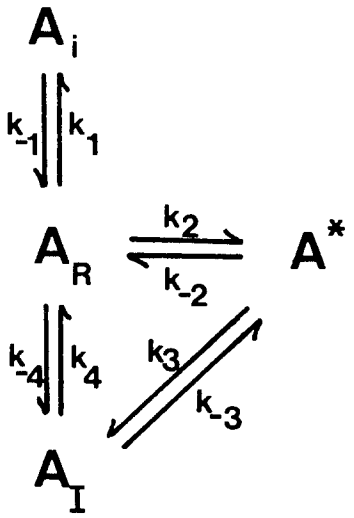

A is the voltage-sensitive molecule in the T tubule membrane and it has a resting conformation A_R. When the membrane field is reduced, the molecule can assume at least three other conformations: an active form, A^*; an inhibited form, A_i; or an inactive form, A_I. The following assumptions are necessary to explain the data presented above:

(*a*) The rate constants k_1, k_2, k_{-2}, k_3, and k_4 are voltage dependent.

(*b*) Contraction threshold depends upon the formation of a critical concentration of A^*. The threshold concentration of A^* is achieved more rapidly for large depolarizations than for small depolarizations as shown by the strength-duration curve (i.e., for soleus fibers the threshold concentration is achieved in 5 ms with a depolarization to −45 mV or in 500 ms with depolarization to −60 mV; Dulhunty, 1980).

(*c*) If k_2 and k_{-2} are given appropriate values, the concentration of A_i can rapidly reach a steady-state value (i.e., within 10 ms; see Fig. 2) after depolarization.

(*d*) The value of k_3 is small and depolarization must be maintained for several seconds before a significant fraction of A is converted to A_I (see Fig. 9 C). The rate constant k_4 has a negative voltage sensitivity so that A is trapped in the A_I conformation until the membrane is repolarized. The rate constants k_{-3} and k_{-4} are infinitely small.

In the experiment illustrated in Fig. 2 B, a 2-ms test pulse reached contraction threshold with a depolarization to −40 mV. When the test pulse was preceded by a 5-mV depolarization, lasting 10–100 ms, inhibition was apparent and the 2-ms test pulse did not reach contraction threshold until the membrane was depolarized to −38 mV. This observation can be explained in terms of the model in the following way. When the test pulse was applied alone the threshold concentration of A^* was reached after 2 ms with a depolarization to −40 mV. When a 5-mV conditioning depolarization was used the concentration of A^* was negligible after 100 ms, but the concentration of A_R was reduced as the reaction $A_R \rightleftharpoons A_i$ proceeded. Consequently, when the test pulse was applied to the fiber after the conditioning pulse, dA^*/dt was less than it had been with no conditioning pulse, and a greater depolarization was required for A^* to reach to its threshold concentration.

The degree of inhibition was found to increase with larger, brief conditioning depolarizations (to potentials between −75 and −40 mV; see Figs. 2 B and 3), and then to fall as the duration of the depolarization was increased (Figs. 2 B and 4 A and B). In terms of the model, the increase in inhibition with a stronger conditioning depolarization would follow the conversion of a greater fraction of A_R to A_i during the conditioning pulse and a consequent decrease in dA^*/dt during the test pulse. The decline in inhibition with longer conditioning pulses can be attributed to an increase in the concentration of A^* during the pulse and its addition to A^* formed during the test pulse. Thus it was necessary to reduce the amplitude of the test pulse in order to reduce the total concentration of A^* to a threshold value.

Inhibition was not seen with brief conditioning depolarizations to potentials more positive than −40 mV (Figs. 4 B and 5 A) where the conditioning pulse itself reached contraction threshold in <10 ms. Since A_i does not reach a steady-state concentration before 10 ms, it must be assumed that dA^*/dt was very much greater than dA_i/dt, especially during the first 5 ms after depolarization, so that the influence of inhibition was negligible.

When the conditioning depolarization was more positive than −60 mV and maintained for periods of seconds or minutes, inactivation was observed (Figs. 8 and 9 C). During the long depolarization, the reaction $A^* \rightleftharpoons A_I$ proceeded and a significant fraction of A became trapped as A_I.

Another possible explanation for inhibition is that it is a property of the SR. This could only be the case if properties of the SR (other than its Ca conductance) can be altered by a change in the potential difference across the T tubule membrane. Inhibition might occur if the rate of Ca uptake by the SR increased rapidly as a result of T tubule depolarization. However, there is no evidence for a rapid influence of surface membrane potential on SR Ca pump activity.

The role of inhibition in normal muscle function will be difficult to evaluate until its effect on tension output is known. Conditioning and test pulses used to demonstrate inhibition were often similar to an action potential in their size and duration. The influence of inhibition was hidden by activation when large depolarizing conditioning pulses were used and thus inhibition may not have a significant effect on the function of normally healthy muscle. However, it could become significant if the action potential size was less than normal, or if contraction threshold was more positive than normal, as it is in the presence of drugs such as anaesthetic agents (Feinstein, 1963; Almers and Best, 1976).

SUMMARY

The effect of subthreshold depolarization on mechanical threshold was investigated in tetrodotoxin-poisoned mammalian and amphibian skeletal muscle fibers using a two-microelectrode voltage-clamp technique. Mechanical threshold was determined with a 2-ms test pulse.

The immediate effect of depolarization was inhibition of the mechanical system. The consequent increase in test pulse threshold was linearly related to the size of the depolarization and there was, on the average, a 10% increase in threshold for a 10-mV depolarization in mammalian fibers.

The duration of the inhibitory period was also related to the size of the depolarization. Inhibition was interrupted by the onset of activation (seen as a reduction in the test pulse threshold) and, in rat soleus fibers, this occurred within 100 ms with a 20-mV depolarization and within 1 ms with a 40-mV depolarization.

Upon repolarization, inhibition decayed within 10 ms. The decay of activation after brief conditioning pulses was initially rapid (on the average the test pulse threshold recovered to 80% of its control value within 1 ms) and then slow (full recovery took 100–500 ms). After long conditioning pulses, activation often decayed into a period of inhibition.

When depolarization (≥20 mV) was maintained for several seconds the fibers became inactivated. Rat EDL and sternomastoid fibers were strongly inactivated by depolarization to −40 mV and the test pulse to +40 mV did not cause contraction.

I am grateful to Professors Peter Gage and Martin Schneider for their helpful discussion, to Miss M. Dlutowski, Mr. G. Williams, and Mr. Crossley for their technical assistance, and to Mrs. Jean Putnam and Miss Georgina Makaritis for typing the manuscript.
This work was supported by a grant from the Muscular Dystrophy Association of America.

Received for publication 29 June 1981 and in revised form 19 October 1981.

REFERENCES

ADAMS, D. J., S. J. SMITH, and S. H. THOMPSON. 1980. Ionic currents in molluscan soma. *Annu. Rev. Neurosci.* **3**:141–167.

ADRIAN, R. H., W. K. CHANDLER, and A. L. HODGKIN. 1969 *a*. The kinetics of mechanical activation in frog muscle. *J. Physiol. (Lond.)*. **204**:207–230.

ADRIAN, R. H., L. L. COSTANTIN, and L. D. PEACHEY. 1969 *b*. Radial spread of contraction in frog muscle fibers. *J. Physiol. (Lond.)*. **204:**207–230.

ADRIAN, R. H., W. K. CHANDLER, and R. F. RAKOWSKI. 1976. Charge movement and mechanical repriming in skeletal muscle. *J. Physiol. (Lond.)*. **254:**361–388.

ALMERS, W., and P. M. BEST. 1976. Effects of tetracaine on displacement currents and contraction of frog skeletal muscle. *J. Physiol. (Lond.)*. **262:**583–611.

CAPUTO, C. 1972. The time course of potassium contractures of single muscle fibers. *J. Physiol. (Lond.)*. **223:**483–505.

CAPUTO, C., and P. DE BOLANOS. 1979. Membrane potential, contractile activation and relaxation rates in voltage clamped short muscle fibers of the frog. *J. Physiol. (Lond.)*. **289:** 175–189.

CHANDLER, W. K., R. F. RAKOWSKI, and M. F. SCHNEIDER. 1976. Effects of glycerol treatment and maintained depolarization on charge movement in skeletal muscle. *J. Physiol. (Lond.)*. **254:**284–316.

COSTANTIN, L. L. 1974. Contractile activation in frog skeletal muscle. *J. Gen. Physiol.* **63:**657–674.

DULHUNTY, A. F. 1979 *a*. A refractory period after brief activation of mammalian skeletal muscle fibers. *Neurosci. Lett.* **14:**223–228.

DULHUNTY, A. F. 1979 *b*. Distribution of potassium and chloride permeability over the surface and T-tubule membranes of mammalian skeletal muscle. *J. Membr. Biol.* **45:**293–310.

DULHUNTY, A. F. 1980. Potassium contractures and mechanical activation in mammalian skeletal muscles. *J. Membr. Biol.* **57:**223–233.

EISENBERG, R. S., and E. A. JOHNSON. 1970. Three dimensional electrical field problems in physiology. *Prog. Biophys. Mol. Biol.* **20:**1–65.

FEINSTEIN, M. B. 1963. Inhibition of caffeine rigor and radiocalcium movements by local anaesthetics in frog sartorius muscles. *J. Gen. Physiol.* **47:**151–172.

HODGKIN, A. L., and P. HOROWICZ. 1960. Potassium contractures in single muscle fibers. *J. Physiol. (Lond.)*. **153:**386–403.

KOVACS, L., and M. F. SCHNEIDER. 1978. Contractile activation by voltage clamp depolarization of cut skeletal muscle fibers. *J. Physiol. (Lond.)*. **277:**483–506.

PALADE, P. T., and R. L. BARCHI. 1977. Characteristics of chloride conductance in muscle fibers of the rat diaphragm. *J. Gen. Physiol.* **69:**325–342.

SANCHEZ, J. A., and E. STEFANI. 1978. Inward calcium current in twitch muscle fibers of the frog. *J. Physiol. (Lond.)*. **283:**197–209.

SCHNEIDER, M. F., and W. K. CHANDLER. 1973. Voltage dependent charge movement in skeletal muscle: a possible step in excitation-contraction coupling. *Nature (Lond.)*. **242:**244–246.

VALDIOSERA, R., C. CLAUSEN, and R. S. EISENBERG. 1974. Impedence of frog skeletal muscle fibers in various solutions. *J. Gen. Physiol.* **63:**460–471.